Chirality-induced spin current through spiral magnets

Hiroki Watanabe, Koujiro Hoshi, and Jun-ichiro Ohe

Phys. Rev. B **94**, 125143 — Published 23 September 2016

DOI: 10.1103/PhysRevB.94.125143

Chirality-induced spin current through spiral magnets

Hiroki Watanabe, Koujiro Hoshi, and Jun-ichiro Ohe*
Department of Physics, Toho University, 2-2-1 Miyama, Funabashi, Chiba, Japan
(Dated: August 29, 2016)

Spin-polarized current through helimagnets and the conductance modulation due to the chirality mismatch is studied numerically. The one-dimensional spiral magnet structure is obtained by taking into account the Dzyaloshinskii-Moriya Interaction (DMI) and the Ferromagnetic (FM) interaction. Although the spiral magnetic structure consists of the y-z components of the magnetization, the conduction electron through the spiral magnet is polarized in the x direction and its sign depends on the chirality of the spiral structure. We also investigate the charge transport through the junction system consists of two helimagnets. Similar to the giant magnetoresistance in the uniform ferromagnet, the conductance is significantly reduced by attaching the helimagnets with different chiralities. Our proposed mechanism has a possibility of the chirality measuring method by using an electron transport and new type of magnetoresistance using a topological property.

I. INTRODUCTION

Recent developments of spintronics field has revealed that the topological aspect of the local spin configuration induces the nontrivial dynamics of the conduction electrons.[1–6] It is shown that the one-dimensional domain wall is moved by the charge current, so-called spin transfer torque.[7–9] This torque is originated from the additional spin polarization of the conduction electrons which is polarized to the magnetization direction without currents. The inverse effect, *i.e.,* the spin dynamics induced charge current, have also been reported in several magnetic systems with spatial modulations. This spinmotive force is induced by the dynamics of the magnetization chirality.[10–19] It has been pointed out that the nanomagnet with the Dzyaloshinskii-Moriya Interaction (DMI) shows a microscopic magnetic structure with a spin chirality. Not only the one dimensional spiral magnet but also the two dimensional Skyrmion configuration are reported experimentally.[6,20–24] For one dimensional helimagnet system, the chirality is distinguished by the right- and left- handed system which is determined by the sign of the DMI. The spatial configuration of the magnetic component is measured by the well-equipped optical setup.[6] The topological aspect of the nanomagnet is quite useful for developing the spintronics device.

In this paper, we investigate the spin transport through the helimagnet which forms one dimensional spiral structure due to the Dzyaloshinskii-Moriya Interaction (DMI). We obtained the magnetic spiral structure by solving the Landau-Lifshitz-Gilbert equation numerically. Two distinguishable state, the Right-handed system(RHS) and the Left-handed system(LHS) are obtained by choosing the sign of the DMI. The chirality $\lambda = (\vec{M}(\vec{r})\times\vec{M}(\vec{r}+\vec{x}))_x$ is a positive (negative) value for RHS (LHS). By using the obtained magnetic configuration, we calculate the conductance and its polarization in the presence of the exchange interaction between the conduction electrons and the local magnetic moment. The conduction electron is almost polarized in the magnetization direction due to the s-d coupling. Although the spiral structure is formed in the y-z plane, we found that the spin polarization of the conduction electrons has the x component. The sign of this additional spin polarization is determined by the chirality of the helimagnet. The spin polarization becomes larger by increasing the strength of the DMI. Furthermore, we investigate the transport properties of the junction system consists of two helimagnets. Analogous to the giant magneto resistance of the uniform ferromagnet,[26,27] in which the conductance decreases by changing the magnetic configuration from the parallel to the anti-parallel for the magnetic junction system, one can expect that the conductance decreases by attaching the different chirality. Our results shows that the conductance decreases significantly by changing the chirality of the adjacent helimagnet. We found that the decreasing of the conductance is enhanced by controlling the magnetization angle at the interface. Proposed system has a possibility of a chirality measurement without optical setup. The conductance modulation of the chirality mismatch may open the new type of the magnetoresistance in the spintronics field.

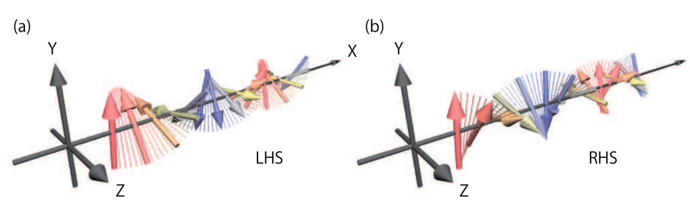

FIG. 1: (color online) Schematic view of the helimagnet. (a) Left-handed system. The chirality ($\lambda = (\vec{M}(\vec{r})\times\vec{M}(\vec{r}+\vec{x}))_x$) is negative. (b) Right-handed system ($\lambda > 0$). The spatial period of the spiral structure is determined by the ratio between the strength of DMI and the strength of the FM. For calculating transport properties, the conduction electrons propagates in the x-direction.

II. MODEL AND METHOD

A. Magnetic configuration

To calculate the electron transport and the spin polarization through the helimagnet, we first solve the Landau-Lifshitz-Gilbert (LLG) equation for obtaining the realistic magnetic configuration. The LLG equation is represented by

$$\frac{\partial \vec{M}(\mathbf{r},t)}{\partial t} = -\gamma \vec{M}(\mathbf{r},t) \times \vec{H}_{\text{eff}} + \frac{\alpha}{M_{\text{s}}} \vec{M}(\mathbf{r},t) \times \frac{\partial \vec{M}(\mathbf{r},t)}{\partial t}, \quad (1)$$

where $\gamma = 1.76 \times 10^{11}$ $\text{T}^{-1}\text{s}^{-1}$ is the gyromagnetic ratio and α is the Gilbert damping coefficient. The effective magnetic field $\vec{H}_{\text{eff}} = -\partial\mathcal{H}/\partial\vec{M}$ is calculated from the classical Heisenberg model,

$$\mathcal{H} = -J_{\text{ex}} \sum_{i,j} \vec{M}_i \cdot \vec{M}_j + D \sum_i (\vec{M}_i \times \vec{M}_{i+\hat{x}} \cdot \hat{x}), \quad (2)$$

where J_{ex} is the exchange interaction energy between nearest neighbours site, D is the strength of the DMI. To obtain the grand state of the magnetic configuration, we start from the random configuration and solve the time evolution of the LLG equation with a large damping coefficient $\alpha = 0.1$. The forth order Runge-Kutta method is employed for solving the LLG equation. We obtain the spiral structure as illustrated in Fig.1. In the present paper, we fixed the stiffness constant A to 10 pJ/m. The unit cell is $5 \times 5 \times 10$ nm^3, and the saturation magnetization M_{s} is 1 T. The special period of the spiral magnet is determined by the ratio D/J_{ex}[6,24]. By using the positive (negative) value of the DMI, we obtain the Right(Left)-handed system.

B. Electron transport through the helimagnet

By using spiral magnetic configuration, we calculate spin-dependent conductance by employing the recursive Green's function method.[28] The Hamiltonian of the conduction electron is expressed by the tight binding model,

$$H = -V_0 \sum_{<i,j>,\sigma} c^\dagger_{i\sigma} c_{j\sigma} - J_{\text{sd}} \sum_{i,\sigma,\sigma'} c^\dagger_{i\sigma} \vec{\hat{\sigma}}_{\sigma,\sigma'} c_{i\sigma'} \cdot \vec{M}_i, \quad (3)$$

where i,j denotes the index of the position. $c_{i\sigma}(c^+_{i\sigma})$ is the annihilation (creation) operator of the i cite with the spin σ. $\vec{M}_i$ is the magnetization of the i cite that is calculated by the LLG equation. $V_0 (= \hbar^2/2m^*a)$ is the transfer energy of the conduction electrons. a is the lattice constant and $m^* = 0.067 m_e$ is the effective mass. We set the lattice constant to 5 nm so that the transfer energy is $V_0 \sim 23$ meV. We employ the 2-dimensional electron gas system, the conduction electron energy (E_F) exists $-4V_0 \leq E_F \leq 4V_0$. The spin polarization of the conduction electrons in the $\nu-$direction is defined as

$$P_\nu = \frac{\text{Tr}\hat{t}^+ \hat{\sigma}^\nu \hat{t}}{\text{Tr}\hat{t}^+ \hat{t}}, \quad (4)$$

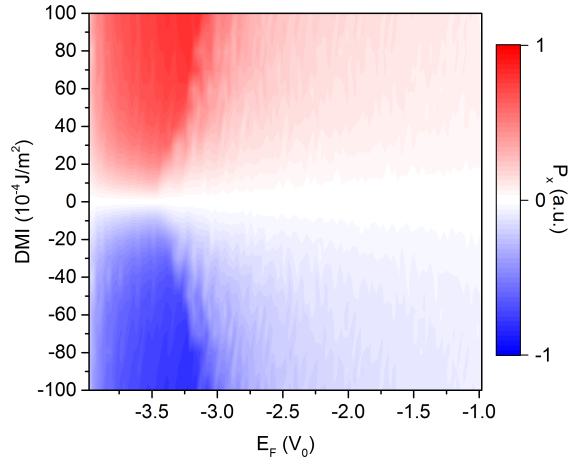

FIG. 2: (color online) The spin polarization of the conduction electron (P_x) through the helimagnet.E_{F} is the Fermi energy of the conduction electrons. For the positive value of the DMI, the helimagnet forms the Right-handed system in the y-z plane. The sign of the P_x is determined by the chirality of the helimagnet.

where $\hat{t}$ is the transmission matrix represented in the 2×2 spin space.

We also calculate the wave packet dynamics of the conduction electrons in the presence of the helimagnet. The time evolution of wave packet is calculated by using the kernel polynomial method[29–31]. The time evolution of the wave function is given by

$$|\psi(\boldsymbol{r}, t + \text{d}t)\rangle = e^{-\text{i}H\text{d}t} |\psi(\boldsymbol{r}, t)\rangle, \quad (5)$$

where $e^{-\text{i}H\text{d}t}$ is the time evolution operator. The time evolution operator $e^{-\text{i}H\text{d}t}$ can be expanded by the Chebyshev polynomials $T_k(H)$ as

$$e^{-\text{i}H\text{d}t} = \sum_{k=0}^{\infty} (2 - \delta_{k0})(-\text{i})^k J_k(\text{d}t) T_k(H) \quad (6)$$

where J_k is the k-th order Bessel function of the first kind. The Chebyshev polynomials $T_k(H)$ is given by

$$T_k(H) = \cos(k \arccos H). \quad (7)$$

$|\psi_k\rangle \equiv T_k(H) |\psi_0\rangle$ is calculated recursively as

$$|\psi_k\rangle = 2H |\psi_{k-1}\rangle - |\psi_{k-2}\rangle. \quad (8)$$

For calculating the first time evolution, one set the ψ_0 as a given initial state and ψ_1 is given by

$$|\psi_1\rangle = H |\psi_0\rangle. \quad (9)$$

We take the summation up tp $k = 30$ in eq.(6) for satisfying the unitarity of the wave function.

III. RESULTS AND DISUCUSSIONS

A. Spin polarized current through the helimagnet

In this section, we discuss the spin polarization of the conduction electrons through the helimagnet. We show the spin polarization P_x of the conduction electrons as a function of the Fermi energy of the conduction electrons E_{F} and the strength of the DMI in Fig. 2. The size of the 2-dimensional system is 300×150 nm^2 and the s-d coupling energy J_{sd} is set to $0.5V_0$. The spiral structure forms in the y-z plane and the sign of the chirality λ is determined by the sign of the DMI strength. In the present calculation, we obtained the Right-Handed System (RHS) for the positive DMI strength. The conduction electron propagates in the x direction. Figure 2 shows that the conduction electrons spin is polarized in the x direction, and the sign of the spin polarization is determined by the chirality of the helimagnet. For the static system without a charge current, the conduction electrons polarizes parallel to the local magnetization. Therefore, this additional spin polarization is due to the non-equilibrium effect driven by the charge current. This additional spin polarization in helimagnets is known as a spin-transfer torque that induces the magnetization dynamics.[9] To understand this additional spin polarization due to the helimagnet, we consider the simple analytical model of the helimagnet structure as

$$\vec{M}(\vec{r}) = M(0, \cos\lambda x, \sin\lambda x), \tag{10}$$

where chirality λ represents the winding period of the spiral structure. The Hamiltonian of the conduction electrons coupling with local magnetic moments is expressed as the new frame of the SU(2) spin space by using unitary transformation U,[4]

$$H' = U^\dagger H U = \frac{(\vec{p} - \vec{\hat{A}})^2}{2m} - J_{\mathrm{ex}}\hat{\sigma}^z M, \tag{11}$$

where $\vec{\hat{A}} = (\mathrm{i}\lambda\hat{\sigma}^x/2, 0, 0)$ is the effective vector potential originated from the unitary transformation $U = \exp(\mathrm{i}\lambda\hat{\sigma}^x x/2)$. The Hamiltonian H' indicates that the conduction spins polarized in the magnetization direction (the z direction in the new flame), and the vector potential $\vec{\hat{A}}$ induces the spin polarization in the x direction when the electron propagates in the x direction. The spin polarization is enhanced by increasing the strength of the DMI as shown in Fig. 2. Because we set the s-d coupling energy to $J_{\mathrm{sd}} = 0.4V_0$, the spin polarization decreases when the Fermi energy of the conduction electron exceeds the s-d coupling energy ($E_{\mathrm{F}} > -3.6V_0$).

We also calculate the time evolution of the wave packet of the conduction electrons through the helimagnet. The initial state is the Gaussian wave packet propagating in the x direction,

$$\psi_\sigma(\boldsymbol{r}, 0) = A\sin\left(\frac{\pi y}{L_y + 1}\right)\exp\left(ik_x x - \frac{\delta k_x^2 x^2}{4}\right)\chi_\sigma^x, \tag{12}$$

where the spinor χ_σ^x is the eigenspinors of the x direction,

$$\chi_\uparrow^x = \frac{1}{\sqrt{2}}\begin{pmatrix}1\\1\end{pmatrix}, \chi_\downarrow^x = \frac{1}{\sqrt{2}}\begin{pmatrix}1\\-1\end{pmatrix}. \tag{13}$$

$L_y = 150$ nm is the width of the 2-dimensional gas system. A is normalization constant obtained by $\langle\psi_\sigma(\boldsymbol{r}, 0)|\psi_\sigma(\boldsymbol{r}, 0)\rangle = 1$ and we set the parameters of the wave packet as $\delta k_x^2 = 0.2$ and $k_x = 0.5$. Figure 3 shows the time evolution of the wave packet in the presence of the helimagnet of the Right-Handed System(RHS). The helimagnet exists 200 nm $\leq x \leq$ 400 nm. We plot both the charge density $C(\boldsymbol{r}, t)$ and spin density of the x direction defined $S_x(\boldsymbol{r}, t)$ as

$$\begin{aligned} C(\boldsymbol{r}, t) &= \sum_\sigma \langle\psi_\sigma(\boldsymbol{r}, t)\psi_\sigma(\boldsymbol{r}, t)\rangle \\ S_x(\boldsymbol{r}, t) &= \sum_\sigma \langle\psi_\sigma(\boldsymbol{r}, t)|\,\hat{\sigma}^x\,|\psi_\sigma(\boldsymbol{r}, t)\rangle. \end{aligned} \tag{14}$$

From the Fig. 3, the additional spin polarization is obtained when the conduction electron propagates in the helimagnet. We also obtained negative spin polarization by using the Left-handed system. These results indicates that the chirality of the helimagnet can be determined by measuring the spin polarization of the conduction electron. However, it requires the optical method or well-fabricated mesoscopic system for measuring the spin polarization of the conduction electrons. To overcome this difficulty, we propose the new method for determining the chirality of the helimagnet by using the charge transport through the junction system in the next section.

B. Conductance modulation due to the chirality mismatch

In this section, we investigate the transport properties for the junction system which consists of two helimagnets. The junction system with different chiralities is naturally obtained in experiments.[25] We consider the conductance modulation due to the switching of the chirality from the RHS/RHS to the RHS/LHS junction. The conductance modulation due to the switching of the relative orientation of the (uniform) magnetic multilayers is known as a giant magnetoresistance (GMR).[26,27] In the GMR systems, the conductance mismatch occurs at the interface due to the spin-dependent chemical potential in each ferromagnetic layer. The relative orientation of the ferromagnet plays an important role for determining the magnetoresistance. It is natural to expect the conductance mismatch also occurs at the interface between helimagnets with different chirality. Fig.4(a) shows the proposed system which consists of two helimagnets. Both helimagnets have the y-z component and we define the angle θ representing the relative angle of two helimagnets at the interface. To prevent the conduction scattering at the interface, we set the magnetization is parallel at

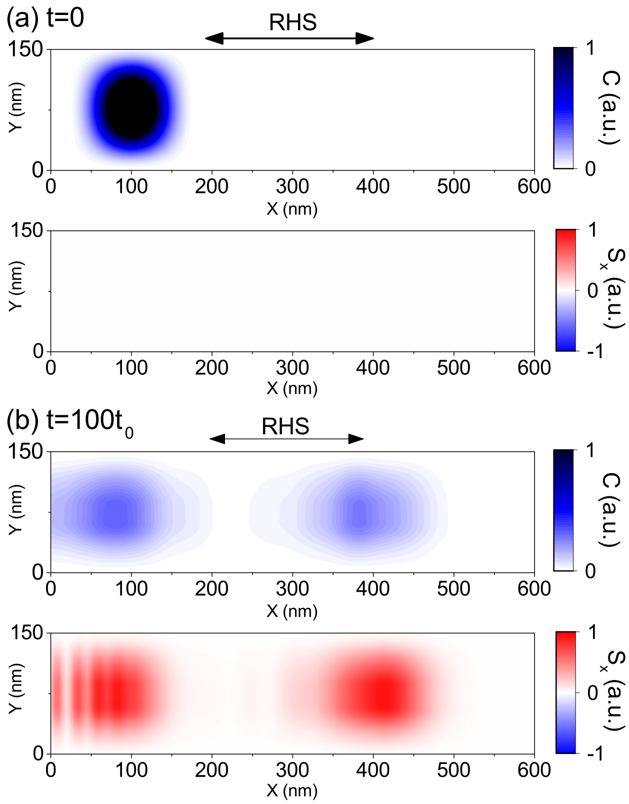

FIG. 3: (color online) Wave packet dynamics thorough the helimagnet. (a) Initial state ($t = 0$) of the wave packet. (b) The wave packet at $t = 100t_0$, where $t_0 (= \hbar/V_0 \sim 0.028$ ps) is the unit time of the calculation.

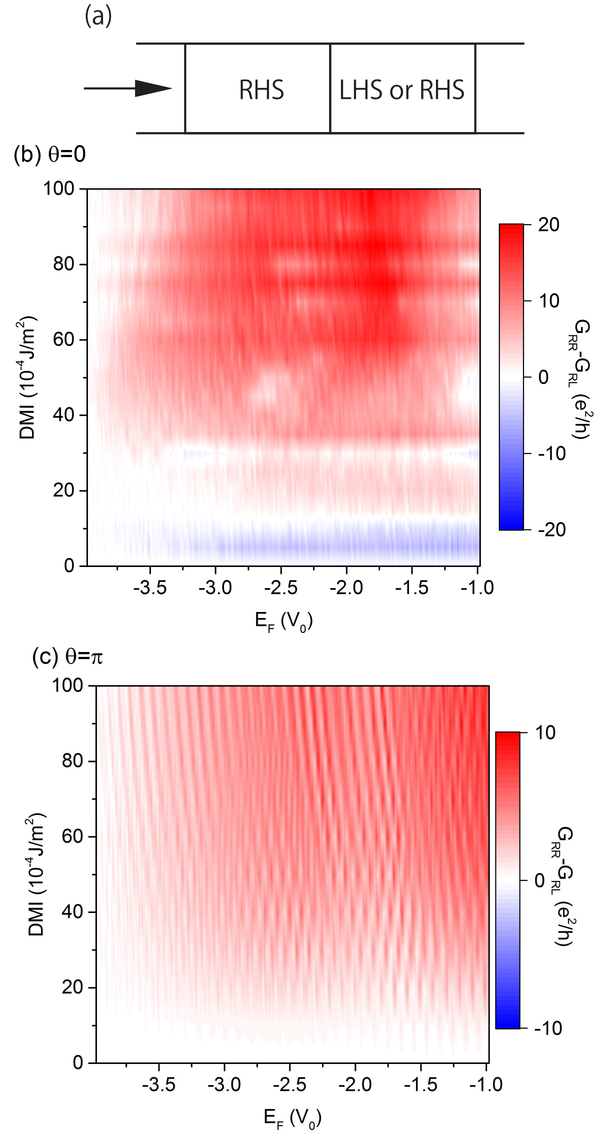

FIG. 4: (color online) (a) Schematic view of the junction system. (b),(c) The conductance modulation $G_{\rm RR} - G_{\rm RL}$ by changing the chirality of the helimagnet in the junction system. The angle at the interface of the junction system is (a) $\theta = 0$ and (b) $\theta = \pi$.

the interface $\theta = 0$. The conductance through the junction system with same (different) chirality is expressed as $G_{\rm RR}(G_{\rm RL})$. Fig. 4 shows the conductance modulation ($G_{\rm RR} - G_{\rm RL}$) as a function of the Fermi energy and the strength of the DMI. The conduction modulation is positive except for the DMI$< 10^{-4}$ J/m^2. This means that the conductance decrease by changing the chirality of the adjacent helimagnet. By increasing the strength of the DMI, the modulation of the conductance becomes large. We found that the negative modulation for the DMI$< 10^{-4}$ J/m^2 is due to the resonant level scattering of the quantum well formed at the center of the junction. For clarifying this effect, we change the magnetization angle at the interface $\theta = \pi$ to prevent forming the quantum well at the interface. Figure 4(c) shows the conductance modulation for the case of $\theta = \pi$. The conductance modulation is positive in the whole energy region and the order is ~ 10 e$^2/h$ that is sufficiently large for measuring in experiments. We note that the conduction reduction can be obtained in whole energy region. Therefore, the proposed mechanism is valid for the wide variety of the material including magnetic metals and magnetic semiconductors. This effect can be measured by the charge conductance and provides the new method for determining the chirality of the helimagnet without the optical technique. We also calculate the wave packet dynamics for the junction system as shown in Fig. 5. The wave packet is reflected at the interface of the RHS/LHS junction system that consists of the conductance calculation.

IV. CONCLUSIONS

We have investigated numerically the spin-polarized conductance through the one dimensional helimagnet. The spiral structure of the helimagnet is obtained by solving the LLG equation with the Dzyaloshinskii-Moriya Interaction(DMI) and the Ferromagnetic coupling(FM).

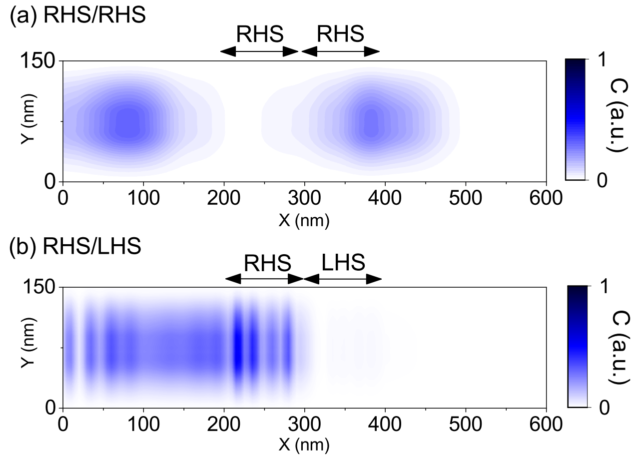

FIG. 5: (color online) Wave packet dynamics thorough the junction system at $t = 100t_0$. The initial state is the same as Fig. 3. The wave packet is reflected at the interface of the junction system RHS/LHS.

We have calculate the spin polarization of the conduction electrons through the helimagnet. The additional spin polarization perpendicular to the magnetization direction has obtained and the sign of the polarization is determined by the chirality of the helimagnet. We have also investigated the conductance property of the junction system consists of two helimagnets. We found that the conductance decreases by changing the the chirality of the adjacent helimagnet from the RHS/RHS to the RHS/LHS, where RHS(LHS) is the Right(LHS)-Handed System. The depression of the conductance becomes larger by increasing the strength of the DMI. The effect has been enhanced by changing the magnetization angle at the interface of the junction system. The wave packet dynamics also show the spin polarization inside the helimagnet and the reflection at the interface of different chirality. Proposed mechanism opens the possibility of measuring the magnetic chirality by using the charge transport and a new type of the magnetoresistance by using the topological quantity of the non-uniform magnet.

Appendix: Spin-dependent transport

The spin-polarization of the conduction electrons is calculated by the spin-resolved Green's function method.[28,32,33] The Green's function including the semi-inifinite ideal lead that has no magnetic moment is defined as

$$\hat{\mathbf{G}} = \frac{1}{\hat{\mathbf{H}} - E\hat{\mathbf{I}} - \hat{\mathbf{\Sigma}}}, \tag{A.1}$$

where $\hat{\mathbf{H}}$ is the matrix representation of the Hamiltonian of the system with magnetic moment represented in Eq. (3), E is the energy of the conduction electrons and $\hat{\mathbf{I}}$ is the unit matrix. $\mathbf{\Sigma}$ is the self-energy due to attach the lead[32]. We consider the system size as $L \times W$ cites, where L is the system length and W is the system width. The normal leads are attached at $x = 0$ and $x = L + 1$ and the electron propagates in the $+x$ direction. By using the amplitude of the wave function $C_i = (C_{i\uparrow}, C_{i\downarrow})^{\mathrm{T}}$ in the spinor expression at the cite i of the x-coordinate, the Eq. (A.1) can be rewritten as

$$\begin{pmatrix} C_0 \\ C_1 \\ \vdots \\ C_{N+1} \end{pmatrix} = \begin{pmatrix} \hat{\mathbf{G}}_{0,0} & \cdots & \hat{\mathbf{G}}_{0,N+1} \\ \vdots & \ddots & \vdots \\ \hat{\mathbf{G}}_{N+1,0} & \cdots & \hat{\mathbf{G}}_{N+1,N+1} \end{pmatrix} \times \begin{pmatrix} \hat{\mathbf{U}}\left(\hat{\mathbf{\Lambda}} - \hat{\mathbf{\Lambda}}^{-1}\right)\hat{\mathbf{U}}^{\dagger} C_0 \,(+) \\ 0 \\ \vdots \\ 0 \end{pmatrix}, \tag{A.2}$$

where $\hat{\mathbf{U}}$ is consisted from the eigenmode of the wave-function in y-direction $\mathbf{u}_1, \cdots \mathbf{u}_M$ as

$$\hat{\mathbf{U}} = (\mathbf{u}_1, \cdots \mathbf{u}_M). \tag{A.3}$$

$\hat{\mathbf{\Lambda}}$ is the diagonal matrix represented as

$$\hat{\Lambda} = \begin{pmatrix} \exp(ik_1) & \cdots & 0 \\ \vdots & \ddots & \vdots \\ 0 & \cdots & \exp(ik_M) \end{pmatrix}, \tag{A.4}$$

where k_j is the wave vector of j-th mode. The transmission coefficient from the i-th mode of the spin σ to the j-th mode of the spin σ' is given by

$$t_{j\sigma',i\sigma} = \sqrt{\frac{v_j}{v_i}} \left(\hat{\mathbf{U}}^{\dagger}\hat{\mathbf{G}}_{N+1,0}\hat{\mathbf{U}}\left(\hat{\mathbf{\Lambda}}^{-1} - \hat{\mathbf{\Lambda}}\right)\right)_{j\sigma',i\sigma}, \tag{A.5}$$

where v_i is the velocity of the i-th mode. By using these spin-resolved transmission coefficient, the transmission matrix is represented as

$$\hat{t}_{ij} = \begin{pmatrix} t_{i\uparrow,j\uparrow} & t_{i\downarrow,j\uparrow} \\ t_{i\uparrow,j\downarrow} & t_{i\downarrow,j\downarrow} \end{pmatrix}. \tag{A.6}$$

The conductance from the j-th mode to the i-th mode is given by $G = (e^2/h)\mathrm{Tr}\hat{t}_{ij}^{\dagger}\hat{t}_{ij}$, and the poralization of the conduction electrons is given by Eq.(4).

Acknowledgments

The authors are grateful to T. Kawarabayashi, Y. Togawa and T. Ohtsuki for valuable discussions. This work was supported by CREST, JST. Grant-in-Aids from the Ministry of Education, Culture, Sports, Science and Technology of Japan (Grants No. 26108715).

* junichirou.ohe@sci.toho-u.ac.jp

[1] N. Nagaosa, J. Sinova, S. Onoda, A. H. MacDonald, and N. P. Ong, Rev. Mod. Phys. **82,** 1539 (2010).
[2] A. Neubauer, C. Pfleiderer, B. Binz, A. Rosch, R. Ritz, P. G. Niklowitz, and P. Böni, Phys. Rev. Lett. **102,** 186602 (2009).
[3] K. Yasuda, R. Wakatsuki, T. Morimoto, R. Yoshimi, A. Tsukazaki, K. S. Takahashi, M. Ezawa, M. Kawasaki, N. Nagaosa and Y. Tokura, Nature Physics **12,** 555 (2016).
[4] G. Tatara, H. Kohno, J. Shibata, Y. Lemaho, and K. -J. Lee, J. Phys. Soc. Jpn. **76,** 054707 (2007).
[5] A. S. Ovchinnikov, Vl. E. Sinitsyn, I. G. Bostrem, J. Kishine, J. Exp. and Theor. Phys. **116,** 791 (2013).
[6] Y. Togawa, Y. Kousaka, S. Nishihara, K. Inoue, J. Akimitsu, A. S. Ovchinnikov, and J. Kishine, Phys. Rev. Lett. **111,** 197204 (2013).
[7] J. C. Slonczewski, J. Magn. Magn. Mater. 159, L1 (1996).
[8] L. Berger, J. Appl. Phys. **3,** 2156 (1978); L. Berger, J. Appl. Phys. **3** 2137 (1979).
[9] G. Tatara and H. Kohno, Phys. Rev. Lett. **92,** 086601 (2004).
[10] A. Stern, Phys. Rev. Lett. **68**, 1022 (1992).
[11] S. E. Barnes and S. Maekawa, Phys. Rev. Lett. **98**, 246601 (2007).
[12] J. Ohe and S. Maeakawa, J. Appl. Phys. **105,** 07C706 (2009).
[13] J. Ohe, S. E. Barnes, H. -W. Lee, and S. Maekawa, Appl. Phys. Lett. **95,** 123110 (2009).
[14] S. A. Yang, G. S. D. Beach, C. Knutson, D. Xiao, Z. Zhang, M. Tsoi, Q. Niu, A. H. MacDonald, and J. L. Erskine: Phys. Rev. B **82,** 054410 (2010).
[15] Y. Yamane, K. Sasage, T. An, K. Harii, J. Ohe, J. Ieda, S. E. Barnes, E. Saitoh, and S. Maekawa, Phys. Rev. Lett. **107,** 236602 (2011).
[16] K. Tanabe, D. Chiba, J. Ohe, S. Kasai, H. Kohno, S. E. Barnes, S. Maekawa, K. Kobayashi and T. Ono, Nature Communications **3,** 845 (2012).
[17] J. Kishine, I. Bostrem, A. S. Ovchinnikov, and Vl. E. Sinitsyn, Phys. Rev. B **86,** 214426 (2012).
[18] K. -W. Kim, J. -H. Moon, K. -J. Lee and H. -W. Lee, Phys. Rev. Lett. **108,** 217202 (2012).
[19] G. E. Volovik: J. Phys. C **20,** L83 (1987).
[20] X. Z. Yu, Y. Onose, N. Kanazawa, J. H. Park, J. H. Han, Y. Matui, N. Nagaosa, and Y. Tokura, Nature **465,** 901 (2010).
[21] X. Z. Yu, N. Kanazawa, Y. Onose, K. Kimoto, W. Z. Zhang, S. Ishikawa, Y. Matui and Y. Tokura, Nature Mater. **10,** 106 (2010).
[22] M. Mochizuki, Phys. Rev. Lett. **108,** 017601 (2012).
[23] S. Mühlbauer, B, Binz, F. Jonietz, C. Pfleiderer, A. Rosch, A. Neubauer, R. Georgii, P. Böni, Science **323,** 915 (2009).
[24] S. Rohart and A. Thiaville, Phys. Rev. B **88,** 184422 (2013).
[25] Y. Togawa, *et. al.,* Phys. Rev. B **92,** 220412(R) (2015).
[26] G. Binasch, P. Grunberg, F. Saurenbach, and W. Zinn, Phys. Rev. B **39,** 4828(R) (1989).
[27] M. N. Baibich, J. M. Broto, A. Fert, F. Nguyen Van Dau, F. Petroff, P. Etienne, G. Creuzet, A. Friederich, and J. Chazelas, Phys. Rev. Lett. **61,** 2472 (1988).
[28] T. Ando, Phys. Rev. B **44,** 8017 (1991).
[29] A. Weiße, G. Wellein, A. Alvermann and H. Fehske, Rev. Mod. Phys. **78,** 275 (2006).
[30] H. Tal-Ezar and R. Kosloff, J. Chem. Phys. **81,** 3967 (1984).
[31] R. Chen and H. Guo, J. Comp. Phys. Commun. **119,** 19 (1999).
[32] S. Datta, *"Electronic Transport in Mesoscopic Systems"* Cambridge Unversity Press, 1995.
[33] J. Ohe, T. Ohtsuki, and B. Kramer, Phys. Rev. B **75,** 245313 (2007).